

## Quantum chaos: An introduction via chains of interacting spins 1/2

Aviva Gubin and Lea F. Santos

Citation: *Am. J. Phys.* **80**, 246 (2012); doi: 10.1119/1.3671068

View online: <http://dx.doi.org/10.1119/1.3671068>

View Table of Contents: <http://ajp.aapt.org/resource/1/AJPIAS/v80/i3>

Published by the American Association of Physics Teachers

---

### Related Articles

Five popular misconceptions about osmosis

*Am. J. Phys.* **80**, 694 (2012)

Resource Letter SS-1: The Spin-Statistics Connection

*Am. J. Phys.* **80**, 561 (2012)

Introducing thermodynamics through energy and entropy

*Am. J. Phys.* **80**, 627 (2012)

Analytic determination of the mean free path of sequential reactions

*Am. J. Phys.* **80**, 316 (2012)

Experiments with a Malkus-Lorenz water wheel: Chaos and Synchronization

*Am. J. Phys.* **80**, 192 (2012)

---

### Additional information on Am. J. Phys.

Journal Homepage: <http://ajp.aapt.org/>

Journal Information: [http://ajp.aapt.org/about/about\\_the\\_journal](http://ajp.aapt.org/about/about_the_journal)

Top downloads: [http://ajp.aapt.org/most\\_downloaded](http://ajp.aapt.org/most_downloaded)

Information for Authors: <http://ajp.dickinson.edu/Contributors/contGenInfo.html>

## ADVERTISEMENT



# Quantum chaos: An introduction via chains of interacting spins 1/2

Aviva Gubin and Lea F. Santos<sup>a)</sup>

*Department of Physics, Yeshiva University, 245 Lexington Avenue, New York, New York 10016*

(Received 27 June 2011; accepted 29 November 2011)

We introduce aspects of quantum chaos by analyzing the eigenvalues and the eigenstates of quantum many-body systems. The properties of quantum systems whose classical counterparts are chaotic differ from those whose classical counterparts are not chaotic. The spectrum of the first exhibits repulsion of the energy levels, which is one of the main signatures of quantum chaos. We show how level repulsion develops in one-dimensional systems of interacting spins 1/2 which are devoid of random elements and involve only two-body interactions. In addition to the statistics of the eigenvalues, we analyze how the structure of the eigenstates may indicate chaos. The programs used to obtain the data are available online. © 2012 American Association of Physics Teachers. [DOI: 10.1119/1.3671068]

## I. INTRODUCTION

Classical chaos is related to the extreme sensitivity of the dynamics of a system to its initial conditions, a concept that can be traced back to Poincaré.<sup>1</sup> The main features of classical chaos can be illustrated by a dynamical billiard, which is an idealized billiard table with no friction where a particle reflects elastically from boundaries which can have any shape. The motion of the particle is represented in phase space by a trajectory, whose evolution is restricted to a surface of constant energy. Depending on the shape of the boundaries, the system may be chaotic, which means that two trajectories whose initial conditions are very close will diverge exponentially in time. The rate of this separation is characterized by the Lyapunov exponent.<sup>2</sup> The trajectories may also become ergodic, which implies that after a long time the particle will have visited the entire surface of constant energy. Equivalently, we may say that after a long time, the particle is equally likely to be found in any point of the accessible phase space.

For quantum systems, the notion of phase-space trajectories loses its meaning as can be seen from the Heisenberg uncertainty principle. Nevertheless, because classical physics is a limit of quantum physics, it is natural to search for quantum signatures of classical chaos. The relation between quantum mechanics and classical chaos is the subject of quantum chaos.<sup>3–5</sup>

Quantum chaos is a very broad field. Our intention is not to review the entire field, but to focus on a particular aspect of it, namely, the spectral statistics and structures of eigenstates of quantum many-body systems as they transition from the regular to the chaotic domain. As a preparation for our goal, we first give a brief idea of some of the important topics of the field (more details are in Refs. 6–9 and in the references to be cited).

Quantum chaos encompasses semiclassical theories aiming at establishing direct links between the trajectories of classically chaotic systems and the properties of these systems in the quantum domain. The main advances in this area were achieved by periodic-orbit theory, which provides a way to calculate the spectrum of a quantum system from its classical periodic orbits (trajectories that repeat themselves after a certain time.) An excellent introduction to the subject was given by Gutzwiller.<sup>4</sup> Gutzwiller's method allowed for the development of a theory of "scars,"<sup>9,10</sup> which refer to the structure of eigenstates that concentrate along the classical

periodic orbits of chaotic systems. Scars were systematically studied by Heller,<sup>11</sup> and the first experimental observations occurred in quantum billiards.<sup>3</sup> Quantum billiards obey the laws of quantum mechanics and correspond to miniature versions of dynamical billiards.

Another important step in the understanding of quantum chaos came from the verification that the distribution of the spacings between neighboring energy levels of a quantum billiard depend on the billiard's classical counterpart.<sup>5,12–14</sup> If the latter is chaotic, the energy levels are highly correlated and repel each other; if it is regular (integrable), the energy levels are uncorrelated, randomly distributed, and can cross.

Level repulsion is one of the main features of quantum chaos. It has been observed in other quantum systems, such as atoms in strong magnetic fields<sup>3</sup> and systems of coupled particles.<sup>7–9,15</sup> Interestingly, level repulsion has been associated also with distributions of prime numbers.<sup>16</sup>

In this article, we focus on quantum many-body systems. A common approach when dealing with such systems is to ignore the details of the interactions and treat them statistically with random matrices. The idea is that when the interactions are strong and the behavior of the system is sufficiently complex, generic properties should emerge. This approach was taken by Wigner<sup>17</sup> to describe the spectrum of heavy nuclei. He employed matrices with random elements, whose only constraint was to satisfy the symmetries of the system. The level spacing distributions of these matrices showed level repulsion and agreed surprisingly well with the data from actual nuclei spectra. When level repulsion was later verified in billiards, a connection between quantum chaos and random matrices became established. Soon after the introduction of random matrices in nuclear physics, they were employed in the analysis of the spectrum of other quantum many-body systems, such as atoms, molecules, and quantum dots.<sup>7–9,15,18,19</sup>

The application of random matrix theory is not restricted to the statistics of eigenvalues but accommodates also studies of eigenstates. Eigenstates of random matrices are pseudo-random vectors; that is, their amplitudes are random variables.<sup>20,21</sup> All the eigenstates are statistically similar, they spread through all basis vectors with no preferences and are therefore ergodic.

Despite the success of random matrix theory in describing spectral statistical properties, it cannot capture the details of real quantum many-body systems. The fact that random matrices are completely filled with statistically independent

elements implies infinite-range interactions and the simultaneous interaction of many particles. Real systems have few-body (most commonly only two-body) interactions which are usually finite range. A better picture of systems with finite-range interactions is provided by banded random matrices, which were also studied by Wigner.<sup>22</sup> Their off-diagonal elements are random and statistically independent but are non-vanishing only up to a fixed distance from the diagonal. There are also ensembles of random matrices that take into account the restriction to few body interactions, so that only the elements associated with those interactions are nonzero; an example is the two-body-random-ensemble<sup>23–25</sup> (see reviews in Refs. 21 and 26). Other models which describe systems with short-range and few-body interactions do not include random elements, such as nuclear shell models,<sup>27</sup> and the systems of interacting spins which we consider in this article.

All the matrices we have mentioned can lead to level repulsion, but differences are observed. For instance, eigenstates of random matrices are completely spread (delocalized) in any basis, whereas the eigenstates of systems with few-body interactions delocalize only in the middle of the spectrum.<sup>26–30</sup>

In this paper, we study a one-dimensional system of interacting spins  $1/2$ . The system involves only nearest-neighbor interactions, and in some cases, also next-nearest-neighbor interactions. Depending on the strength of the couplings, the system may develop chaos, which is identified by calculating the level spacing distribution. We also compare the level of delocalization of the eigenstates in the integrable and chaotic domains. It is significantly larger in the latter case, where the most delocalized states are found in the middle of the spectrum.

The paper is organized as follows. Section II provides a detailed description of the Hamiltonian of a spin  $1/2$  chain. Section III explains how to compute the level spacing distribution and how to quantify the level of delocalization of the eigenstates. Section IV shows how the mixing of symmetries may erase level repulsion even when the system is chaotic. Final remarks are given in Sec. V.

## II. SPIN-1/2 CHAIN

We study a one-dimensional spin  $1/2$  system (a spin  $1/2$  chain) described by the Hamiltonian

$$H = H_z + H_{\text{NN}}, \quad (1a)$$

where

$$H_z = \sum_{i=1}^L \omega_i S_i^z = \left( \sum_{i=1}^L \omega S_i^z \right) + \epsilon_d S_d^z, \quad (1b)$$

$$H_{\text{NN}} = \sum_{i=1}^{L-1} [J_{xy} (S_i^x S_{i+1}^x + S_i^y S_{i+1}^y) + J_z S_i^z S_{i+1}^z]. \quad (1c)$$

We have set  $\hbar$  equal to 1,  $L$  is the number of sites,  $S_i^{x,y,z} = \sigma_i^{x,y,z}/2$  are the spin operators at site  $i$ , and  $\sigma_i^{x,y,z}$  are the Pauli matrices. The term  $H_z$  gives the Zeeman splitting of each spin  $i$ , as determined by a static magnetic field in the  $z$  direction. All sites are assumed to have the same energy splitting  $\omega$ , except a single site  $d$ , whose energy splitting  $\omega + \epsilon_d$  is caused by a magnetic field slightly larger than the

field applied on the other sites. This site is referred to as a defect.

A spin in the positive  $z$  direction (up) is indicated by  $|\uparrow\rangle$  or by the vector  $\begin{pmatrix} 1 \\ 0 \end{pmatrix}$ ; a spin in the negative  $z$  direction (down) is represented by  $|\downarrow\rangle$  or  $\begin{pmatrix} 0 \\ 1 \end{pmatrix}$ . An up spin on site  $i$  has energy  $+\omega_i/2$ , and a down spin has energy  $-\omega_i/2$ . A spin up corresponds to an excitation.

The second term,  $H_{\text{NN}}$ , is known as the XXZ Hamiltonian. It describes the couplings between nearest-neighbor (NN) spins;  $J_{xy}$  is the strength of the flip-flop term  $S_i^x S_{i+1}^x + S_i^y S_{i+1}^y$ , and  $J_z$  is the strength of the Ising interaction  $S_i^z S_{i+1}^z$ . The flip-flop term exchanges the position of neighboring up and down spins according to

$$J_{xy} (S_i^x S_{i+1}^x + S_i^y S_{i+1}^y) |\uparrow_i \downarrow_{i+1}\rangle = (J_{xy}/2) |\downarrow_i \uparrow_{i+1}\rangle, \quad (2)$$

or, equivalently, it moves the excitations through the chain. We have assumed open boundary conditions as indicated by the sum in  $H_{\text{NN}}$  which goes from  $i=1$  to  $L-1$ . Hence, an excitation in site 1 (or  $L$ ) can move only to site 2 (or to site  $L-1$ ). Closed boundary conditions, where an excitation in site 1 can move also to site  $L$  (and vice-versa) are mentioned briefly in Sec. IV.

The Ising interaction implies that pairs of parallel spins have higher energy than pairs of anti-parallel spins, that is,

$$J_z S_i^z S_{i+1}^z |\uparrow_i \uparrow_{i+1}\rangle = +(J_z/4) |\uparrow_i \uparrow_{i+1}\rangle, \quad (3)$$

and

$$J_z S_i^z S_{i+1}^z |\uparrow_i \downarrow_{i+1}\rangle = -(J_z/4) |\uparrow_i \downarrow_{i+1}\rangle. \quad (4)$$

For the chain described by Eq. (1) the total spin in the  $z$  direction,  $S^z = \sum_{i=1}^L S_i^z$ , is conserved, that is,  $[H, S^z] = 0$ . This condition means that the total number of excitations is fixed; the Hamiltonian cannot create or annihilate excitations, it can only move them through the chain.

To write the Hamiltonian in matrix form and diagonalize it to find its eigenvalues and eigenstates, we need to choose a basis. The natural choice corresponds to arrays of up and down spins in the  $z$  direction, as in Eqs. (2), (3), and (4). We refer to it as the site basis. In this basis,  $H_z$  and the Ising interaction contribute to the diagonal elements of the matrix, and the flip-flop term leads to the off-diagonal elements.

In the absence of the Ising interaction, the excitations move freely through the chain. In this case, the eigenvalues and eigenstates can be found analytically. The existence of an analytical method to find the spectrum of a system guarantees its integrability. The addition of the Ising interaction eventually leads to the onset of quantum chaos. The source of chaos is the interplay between the Ising interaction and the defect.<sup>31</sup>

To bring the system to the chaotic regime, we set  $J_{xy} = 1$  (arbitrary units), choose  $J_z = \epsilon_d = 0.5$  (arbitrary units), and place the defect on site  $d = \lfloor L/2 \rfloor$ , where  $\lfloor L/2 \rfloor$  stands for the largest integer less than or equal to  $L/2$ . These choices are based on the following factors. (a) The strength of the Ising interaction cannot be much larger than  $J_{xy}$ , because if it were, basis vectors with different numbers of pairs of parallel spins would have very different energies and  $J_{xy}$  would not be able to effectively couple them. For example, the energy difference between  $|\uparrow\uparrow\downarrow\rangle$  and  $|\uparrow\downarrow\uparrow\rangle$  is  $J_z/2$ ; if we had  $J_z \gg J_{xy}$ , the matrix element  $J_{xy}/2$  coupling these two basis vectors would become ineffective. As a result, the eigenstates would involve only a small portion of the basis vectors, which would

mean localized eigenstates and therefore non-chaotic systems. (b) The defect cannot be placed on the edges of the chain, because in this case an analytical solution exists,<sup>32</sup> and the system is therefore still integrable. (c) We cannot have  $\epsilon_d \gg J_{xy}$ , because this case would break the chain in two; that is, an excitation on one side of the chain would not have enough energy to overcome the defect and reach the other side of the chain. In effect, we would be dealing with two independent chains described by the XXZ model, which is integrable.<sup>33,34</sup>

### III. QUANTUM CHAOS

We use the level spacing distribution to identify when the system becomes chaotic. We analyze also what happens to the structure of the eigenstates once level repulsion occurs.

#### A. Level spacing distribution

The distribution  $P(s)$  of the spacings,  $s$ , of neighboring energy levels differs depending on the system.<sup>7,8,15</sup> The energy levels of integrable systems are not correlated and are not prohibited from crossing, so the distribution is Poissonian ( $P$ ),

$$P_P(s) = e^{-s}. \quad (5)$$

In chaotic systems, the eigenvalues become correlated and crossings are avoided. There is level repulsion, and  $P(s)$  is given by the Wigner-Dyson (WD) distribution, as predicted by random matrix theory. The form of the Wigner-Dyson distribution depends on the symmetry properties of the Hamiltonian. Systems with time reversal invariance are described by a Gaussian orthogonal ensemble, which corresponds to an ensemble of real symmetric matrices, whose elements  $H_{ij}$  are independent random numbers chosen from a Gaussian distribution. The average of the elements and the variance satisfy  $\langle H_{ij} \rangle = 0$  and  $\langle H_{ij}^2 \rangle = 1 + \delta_{ij}$ . The level spacing distribution of a Gaussian orthogonal ensemble is given by

$$P_{WD}(s) = \frac{\pi s}{2} e^{-\pi s^2/4}. \quad (6)$$

The Hamiltonian in Eq. (1) is also real and symmetric, so the distribution achieved in the chaotic limit is the same as  $P_{WD}(s)$ . However, our system has only short-range-two-body interactions, so it cannot reproduce all features of the Gaussian orthogonal ensemble. The density of states, for instance, is Gaussian for Eq. (1), but for the Gaussian orthogonal ensemble it has the shape of half of a circle. Interested readers can obtain these forms using the codes provided.<sup>35</sup> Another difference is the structure of the eigenstates, as discussed in Sec. III B. For Gaussian orthogonal ensembles, all the eigenstates are statistically similar and highly delocalized, whereas for the Hamiltonian in Eq. (1), delocalization is restricted to the middle of the spectrum.

To obtain the level spacing distribution, we first need to separate the eigenvalues according to their symmetry sectors (subspaces). If we mix eigenvalues from different symmetry sectors, we cannot achieve a Wigner-Dyson distribution even if the system is chaotic because eigenvalues from different subspaces are independent and therefore uncorrelated, so do not repel each other. We discuss further the danger of mixing eigenvalues from different symmetry sectors in Sec. IV. For the moment, we need to remember only that the

Hamiltonian in Eq. (1) conserves  $S^z$ . This symmetry implies that the Hamiltonian matrix is separated into uncoupled blocks, corresponding to subspaces with a fixed number of spins in the up direction. In the following, we select a particular subspace with  $L/3$  up spins, whose Hamiltonian matrix has therefore dimension  $D = L! / [(L/3)!(L - L/3)!]$ .

The second essential step before computing the spacing distribution is to unfold the spectrum. The procedure consists of locally rescaling the energies, so that the local density of states of the renormalized eigenvalues is 1. This rescaling allows for the comparison of spectra obtained for different parameters and for different systems. There are different ways to unfold the spectrum. A simple and commonly used procedure is to order the spectrum in increasing values of energy; separate it into several smaller sets of eigenvalues; and divide each eigenvalue by the mean level spacing of its particular set. The mean level spacing of the new set of renormalized energies becomes 1. Because the density of states is the number of states in an interval of energy, that is, the reciprocal of the mean level spacing, this procedure also ensures that the local density of states is unity. This procedure is the one we used.<sup>35</sup>

Given the unfolded spacings of neighboring levels, the histogram can now be computed. To compare it with the theoretical curves, the distribution needs to be normalized, so that its total area is equal to 1.

Figure 1 shows the level spacing distribution when the defect is placed on site 1 and on site  $\lfloor L/2 \rfloor$ . The first case corresponds to an integrable model and the distribution is a Poisson; the second case is a chaotic system, so the distribution is Wigner-Dyson.

#### B. Number of principal components

We now investigate how the transition from a Poisson to a Wigner-Dyson distribution affects the structure of the eigenstates. In particular, we study how delocalized they are in both regimes.

To determine the spreading of the eigenstates in a particular basis, we look at their components. Consider an eigenstate  $|\psi_i\rangle$  written in the basis vectors  $|\zeta_k\rangle$  as  $|\psi_i\rangle = \sum_{k=1}^D c_{ik} |\zeta_k\rangle$ . It will be localized if it has the participation of few basis vectors, that is, if a few  $|c_{ik}|^2$  make significant contributions. It will be delocalized if many  $|c_{ik}|^2$  participate with similar values. To quantify this criterion, we use the sum of the square of the probabilities,  $|c_{ik}|^4$  (the sum of the probabilities would not be a good choice, because normalization implies  $\sum_{k=1}^D |c_{ik}|^2 = 1$ ), and define the number of principal components of eigenstate  $i$  as<sup>27,28</sup>

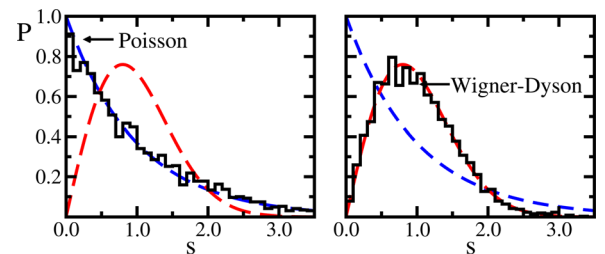


Fig. 1. (Color online) Level spacing distribution for the Hamiltonian in Eq. (1) with  $L = 15$ , 5 spins up,  $\omega = 0$ ,  $\epsilon_d = 0.5$ ,  $J_{xy} = 1$ , and  $J_z = 0.5$  (arbitrary units); bin size = 0.1. (a) Defect on site  $d = 1$ ; (b) defect on site  $d = 7$ . The dashed lines are the theoretical curves.



$$n_i \equiv \frac{1}{\sum_{k=1}^D |c_{ik}|^4}. \quad (7)$$

The number of principal components gives the number of basis vectors which contribute to each eigenstate. It is small when the state is localized and large when the state is delocalized.

For Gaussian orthogonal ensembles, the eigenstates are random vectors, that is, the amplitudes  $c_{ik}$  are independent random variables. These states are completely delocalized. Complete delocalization does not mean, however, that the number of principal components is equal to  $D$ . Because the weights  $|c_{ik}|^2$  fluctuate, the average over the ensemble gives number of principal components  $\sim D/3$ .<sup>27,28</sup>

To study the number of principal components for Eq. (1), we need to choose a basis. This choice depends on the question we want to address. We consider two bases, the site- and mean-field basis. The site-basis is appropriate when analyzing the spatial delocalization of the system. To separate regular from chaotic behavior, a more appropriate basis consists of the eigenstates of the integrable limit of the model, which is known as the mean-field basis.<sup>27</sup> In our case, the integrable limit corresponds to Eq. (1) with  $J_{xy} \neq 0$ ,  $\epsilon_d \neq 0$ , and  $J_z = 0$ .

We start by writing the Hamiltonian in the site-basis. Let us denote these basis vectors by  $|\phi_j\rangle$ . In the absence of the Ising interaction, the diagonalization of the Hamiltonian leads to the mean-field basis vectors. They are given by  $|\xi_k\rangle = \sum_{j=1}^D b_{kj}|\phi_j\rangle$ . The diagonalization of the complete matrix, including the Ising interaction, gives the eigenstates in the site-basis,  $|\psi_i\rangle = \sum_{j=1}^D a_{ij}|\phi_j\rangle$ . If we use the relation between  $|\phi_j\rangle$  and  $|\xi_k\rangle$ , we may also write the eigenstates of the total Hamiltonian in Eq. (1) in the mean-field basis as

$$|\psi_i\rangle = \sum_{k=1}^D \left( \sum_{j=1}^D a_{ij} b_{kj}^* \right) |\xi_k\rangle = \sum_{k=1}^D c_{ik} |\xi_k\rangle. \quad (8)$$

Figure 2 shows the number of principal components for the eigenstates in the site-basis [(a), (b)] and in the mean-field basis [(c), (d)] for the cases where the defect is placed on site 1 [(a), (c)] and on site  $[L/2]$  [(b), (d)]. The level of delocalization increases significantly in the chaotic regime. However, contrary to random matrices, the largest values are restricted

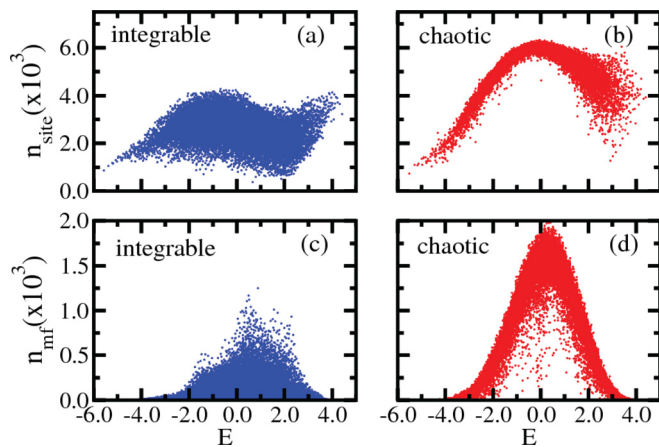


Fig. 2. (Color online) Number of principal components for the eigenstates of the Hamiltonian in Eq. (1) versus energy;  $L=18$ , 6 spins up,  $\omega=0$ ,  $\epsilon_d=0.5$ ,  $J_{xy}=1$ , and  $J_z=0.5$  (arbitrary units). (a) and (b) site-basis; (c) and (d) mean-field basis; (a) and (c) defect on site  $d=1$ ; (b) and (d) defect on site  $d=9$ .

to the middle of the spectrum, the states at the edges being more localized. This property is a consequence of the Gaussian shape of the density of states of systems with two-body interactions. The highest concentration of states appears in the middle of the spectrum, where the strong mixing of states can occur leading to widely distributed eigenstates.

An interesting difference between the integrable and chaotic regimes is the fluctuations of the number of principal components. For the regular system, the number of principal components shows large fluctuations. In contrast, in the chaotic regime, the number of principal components approaches a smooth function of energy. Chaotic eigenstates close in energy have similar structures and consequently similar values of the number of principal components.

#### IV. SYMMETRIES

The presence of a defect breaks symmetries of the system. In this section, we remove the defect and have a closer look at the symmetries.

We refer to the system in the absence of a defect ( $\epsilon_d=0$ ) as defect-free. Contrary to the case where  $\epsilon_d \neq 0$ , a defect-free spin-1/2 chain with NN couplings remains integrable even when the Ising interaction is added. This system can be analytically solved using the Bethe ansatz.<sup>33,34</sup> To drive the system to chaos, while keeping it defect free, we need to add further couplings. By considering couplings between next-nearest-neighbors (NNNs),<sup>36–39</sup> the Hamiltonian becomes

$$H = H_{\text{NN}} + \alpha H_{\text{NNN}}, \quad (9)$$

where

$$H_{\text{NNN}} = \sum_{n=1}^{L-2} \left[ J'_{xy} (S_n^x S_{n+2}^x + S_n^y S_{n+2}^y) + J'_z S_n^z S_{n+2}^z \right]. \quad (10)$$

For sufficiently large  $\alpha$  ( $\alpha \gtrsim 0.2$  for  $L=15$ ), there are various scenarios for which chaos can develop, which include the absence of Ising interactions,  $J_z = J'_z = 0$ ; the absence of the flip-flop term between next-nearest-neighbors,  $J'_{xy} = 0$ ; the absence of Ising interaction between next-nearest-neighbors,  $J'_z = 0$ ; and the presence of all four terms.

Depending on the parameters in Eq. (9), we might not obtain a Wigner-Dyson distribution even if the system is chaotic if not all symmetries of the system are taken into account.<sup>37,39</sup> We have mentioned conservation of total spin in the  $z$  direction. In the absence of a defect other symmetries of  $H$  in Eq. (9) include the following.<sup>40</sup>

##### A. Parity

Parity may be understood by imagining a mirror in one edge of the chain. For eigenstates written in the site-basis, the probability of each basis vector is equal to that of its reflection. For example, suppose we have  $L=4$  and one excitation. The eigenstates are given by  $|\psi_i\rangle = a_{i1} |\uparrow\downarrow\downarrow\downarrow\rangle + a_{i2} |\downarrow\uparrow\downarrow\downarrow\rangle + a_{i3} |\downarrow\downarrow\uparrow\downarrow\rangle + a_{i4} |\downarrow\downarrow\downarrow\uparrow\rangle$ . The amplitudes are either  $a_{i1} = a_{i4}$  and  $a_{i2} = a_{i3}$  for even parity or  $a_{i1} = -a_{i4}$  and  $a_{i2} = -a_{i3}$  for odd parity. The level spacing distribution needs to be independently obtained for each parity.

##### B. Spin reversal

If the chain has an even number of sites and  $L/2$  up spins, then  $S^z = 0$ . In this sector pairs of equivalent basis vectors

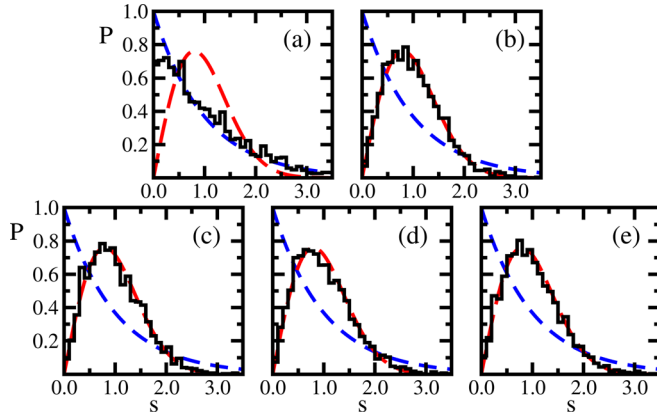


Fig. 3. (Color online) Level spacing distribution for Eq. (9) with  $\alpha=0.5$ ,  $J_{xy}=1$ , and bin size  $=0.1$ . (a)  $L=14$ , 7 spins up,  $J'_{xy}=J_z=J'_z=1$ . All eigenvalues of the subspace  $S^z=0$  are considered. (b)  $J'_{xy}=1$ ,  $J_z=J'_z=0.5$ . (c)  $J'_{xy}=1$ ,  $J_z=J'_z=0$ . (d)  $J'_{xy}=0$ ,  $J_z=J'_z=0.5$ . (e)  $J'_{xy}=1$ ,  $J_z=0.5$ ,  $J'_z=0$ . For (b)–(e)  $L=15$ , 5 spins up. The eigenvalues are separated according to the parity of the corresponding eigenstates.  $P(s)$  is the average of the distributions of the two parity sectors.

correspond to those which become equal if we rotate all the spins from one vector by  $180^\circ$ . For example, state  $|\uparrow\downarrow\uparrow\uparrow\rangle$  pairs with state  $|\downarrow\uparrow\downarrow\downarrow\rangle$ .

### C. Total spin

If the system is isotropic, that is,  $J_{xy}=J_z$  and  $J'_{xy}=J'_z$ , the total spin,  $S^2 = (\sum_{n=1}^L \vec{S}_n)^2$ , is conserved.

For closed boundary conditions, there is also momentum conservation. The more symmetries the system has, the smaller the subspaces become for a given system size, which is not good for statistics. For this reason, we chose open boundary conditions.

In Fig. 3, we show the level spacing distribution for the four chaotic systems we have described. All the figures involve eigenvalues of a single selected  $S^z$ -sector. Both Figs. 3(a) and 3(b) show results for a chaotic spin 1/2 chain with all interactions in Eq. (9) included. Because Fig. 3(a) mixes the three symmetries we have discussed,  $P(s)$  becomes a Poisson distribution, even though the system is chaotic. In Fig. 3(b), just as in Figs. 3(c)–3(e), we circumvent the  $S^z=0$  subspace by avoiding chains with an even number of sites. We also choose  $J_z \neq J_{xy}$  to avoid conservation of total spin. By doing so, the only remaining symmetry is parity, which we take into account. The expected Wigner-Dyson distributions are then obtained.

### V. DISCUSSION

The computer programs used to obtain the data for Figs. 1, 2, and 3 are available.<sup>35</sup> The reader will also find programs to study Gaussian orthogonal ensembles and suggestions for other investigations.

Spin 1/2 chains are excellent models for introducing students to some of the basic concepts of linear algebra, quantum mechanics, as well as to current areas of research. In addition to the crossover from integrability to chaos, they can be used to introduce topics as diverse as the metal-insulator transition, quantum phase transition, entanglement,<sup>41</sup> spintronics, and methods of quantum control.<sup>42</sup> They have been considered as models for quantum computers<sup>43</sup> and magnetic compounds<sup>44</sup> and recently have been simulated in optical lattices.<sup>45–47</sup>

### ACKNOWLEDGMENTS

A.G. thanks Stern College for Women of Yeshiva University for a summer fellowship and the Kressel Research Scholarship for a one-year financial support. This work is part of her thesis for the S. Daniel Abraham Honors Program. L.F.S. thanks M. Edelman, F. M. Izrailev, A. Small, and F. Zypman for useful discussions.

<sup>a</sup>Electronic mail: lsantos2@yu.edu

<sup>1</sup>H. Poincaré, *Science and Method* (Thomas Nelson and Sons, London, 1914).

<sup>2</sup>J. Gleick, *Chaos: Making a New Science* (Viking, New York, 1987).

<sup>3</sup>R. V. Jensen, “Quantum chaos,” *Nature* (London) **355**, 311–318 (1992).

<sup>4</sup>M. C. Gutzwiller, “Quantum chaos,” *Sci. Am.* **206**(1), 78–84 (1992).

<sup>5</sup>Z. Rudnick, “Quantum chaos?,” *Noti. Am. Math. Soc.* **55**(1), 32–34 (2008).

<sup>6</sup>M. C. Gutzwiller, *Chaos in Classical and Quantum Mechanics* (Springer-Verlag, New York, 1990).

<sup>7</sup>F. Haake, *Quantum Signatures of Chaos* (Springer-Verlag, Berlin, 1991).

<sup>8</sup>L. E. Reichl, *The Transition to Chaos: Conservative Classical Systems and Quantum Manifestations* (Springer, New York, 2004).

<sup>9</sup>H.-J. Stöckmann, *Quantum Chaos: An Introduction* (Cambridge U.P., Cambridge, 2007).

<sup>10</sup>M. V. Berry, “Quantum scars of classical closed orbits in phase space,” *Proc. R. Soc. Lond. A* **423**, 219–231 (1989).

<sup>11</sup>E. J. Heller, “Bound-state eigenfunctions of classically chaotic Hamiltonian systems: Scars of periodic orbits,” *Phys. Rev. Lett.* **53**, 1515–1518 (1984).

<sup>12</sup>S. W. McDonald and A. N. Kaufman, “Spectrum and eigenfunctions for a Hamiltonian with stochastic trajectories,” *Phys. Rev. Lett.* **42**, 1189–1191 (1979).

<sup>13</sup>M. V. Berry, “Quantizing a classically ergodic system: Sinai’s billiard and the KKR method,” *Ann. Phys. (NY)* **131**, 163–216 (1981).

<sup>14</sup>O. Bohigas, M. J. Giannoni, and C. Schmit, “Characterization of chaotic quantum spectra and universality of level fluctuation laws,” *Phys. Rev. Lett.* **52**, 1–4 (1984).

<sup>15</sup>T. Guhr, A. Mueller-Gröeling, and H. A. Weidenmüller, “Random matrix theories in quantum physics: Common concepts,” *Phys. Rep.* **299**, 189–425 (1998).

<sup>16</sup>T. Timmerlake, “Random numbers and random matrices: Quantum chaos meets number theory,” *Am. J. Phys.* **74**, 547–553 (2006).

<sup>17</sup>E. P. Wigner, “On the statistical distribution of the widths and spacings of nuclear resonance levels,” *Proc. Cambridge Phil. Soc.* **47**, 790–798 (1951).

<sup>18</sup>C. W. J. Beenakker, “Random-matrix theory of quantum transport,” *Rev. Mod. Phys.* **69**, 731–808 (1997).

<sup>19</sup>Y. Alhassid, “The statistical theory of quantum dots,” *Rev. Mod. Phys.* **72**, 895–968 (2000).

<sup>20</sup>M. V. Berry, “Regular and irregular semiclassical wavefunctions,” *J. Phys. A* **10**, 2083–2091 (1977).

<sup>21</sup>T. A. Brody, J. Flores, J. B. French, P. A. Mello, A. Pandey, and S. S. M. Wong, “Random matrix physics: Spectrum and strength fluctuations,” *Rev. Mod. Phys.* **53**, 385–480 (1981).

<sup>22</sup>E. P. Wigner, “Characteristic vectors of bordered matrices with infinite dimension,” *Ann. Phys.* **62**, 548–564 (1955).

<sup>23</sup>J. B. French and S. S. M. Wong, “Validity of random matrix theories for many-particle systems,” *Phys. Lett. B* **33**, 449–452 (1970).

<sup>24</sup>O. Bohigas and J. Flores, “Two-body random Hamiltonian and level density,” *Phys. Lett. B* **34**, 261–263 (1971).

<sup>25</sup>J. Flores, M. Horoi, M. Müller, and T. H. Seligman, “Spectral statistics of the two-body random ensemble revisited,” *Phys. Rev. E* **63**, 026204 (2001).

<sup>26</sup>V. K. B. Kota, “Embedded random matrix ensembles for complexity and chaos in finite interacting particle systems,” *Phys. Rep.* **347**, 223–288 (2001).

<sup>27</sup>V. Zelevinsky, B. A. Brown, N. Frazier, and M. Horoi, “The nuclear shell model as a testing ground for many-body quantum chaos,” *Phys. Rep.* **276**, 85–174 (1996).

<sup>28</sup>F. M. Izrailev, “Simple models of quantum chaos—Spectrum and eigenfunctions,” *Phys. Rep.* **196**, 299–392 (1990).

<sup>29</sup>G. Casati, B. V. Chirikov, I. Guarneri, and F. M. Izrailev, “Band-random-matrix model for quantum localization in conservative systems,” *Phys. Rev. E* **48**, R1613–R1616 (1993).

- <sup>30</sup>V. V. Flambaum, A. A. Gribakina, G. F. Gribakin, and M. G. Kozlov, "Structure of compound states in the chaotic spectrum of the Ce atom: Localization properties, matrix elements, and enhancement of weak perturbations," *Phys. Rev. A* **50**, 267–296 (1994).
- <sup>31</sup>L. F. Santos, "Integrability of a disordered Heisenberg spin-1/2 chain," *J. Phys. A* **37**, 4723–4729 (2004).
- <sup>32</sup>F. C. Alcaraz, M. N. Barber, M. T. Batchelor, R. J. Baxter, and G. R. W. Quispel, "Surface exponents of the quantum XXZ, Ashkin-Teller and Potts models," *J. Phys. A* **20**, 6397–6409 (1987).
- <sup>33</sup>H. A. Bethe, "On the theory of metal I. Eigenvalues and eigenfunctions of a linear chain of atoms," *Z. Phys.* **71**, 205–217 (1931).
- <sup>34</sup>M. Karbach and G. Müller, "Introduction to the Bethe ansatz I," *Comput. Phys.* **11**, 36–44 (1997).
- <sup>35</sup>See the supplementary material at <http://dx.doi.org/10.1119/1.3671068> for codes written in Mathematica and Fortran to obtain the figures from the paper and also to solve additional exercises.
- <sup>36</sup>T. C. Hsu and J. C. Angles d'Auriac, "Level repulsion in integrable and almost-integrable quantum spin models," *Phys. Rev. B* **47**, 14291–14296 (1993).
- <sup>37</sup>K. Kudo and T. Deguchi, "Level statistics of XXZ spin chains with discrete symmetries: Analysis through finite-size effects," *J. Phys. Soc. Jpn.* **74**, 1992–2000 (2005).
- <sup>38</sup>L. F. Santos and M. Rigol, "Onset of quantum chaos in one-dimensional bosonic and fermionic systems and its relation to thermalization," *Phys. Rev. E* **81**, 036206-1 (2010).
- <sup>39</sup>L. F. Santos, "Transport and control in one-dimensional systems," *J. Math. Phys.* **50**, 095211 (2009).
- <sup>40</sup>W. G. Brown, L. F. Santos, D. J. Starling, and L. Viola, "Quantum chaos, localization, and entanglement in disordered Heisenberg models," *Phys. Rev. E* **77**, 021106 (2008).
- <sup>41</sup>L. Amico, R. Fazio, A. Osterloh, and V. Vedral, "Entanglement in many-body systems," *Rev. Mod. Phys.* **80**, 517–576 (2008).
- <sup>42</sup>L. M. K. Vandersypen and I. L. Chuang, "NMR techniques for quantum control and computation," *Rev. Mod. Phys.* **76**, 1037–1069 (2005).
- <sup>43</sup>B. E. Kane, "A silicon-based nuclear spin quantum computer," *Nature (London)* **393**, 133–137 (1998).
- <sup>44</sup>A. V. Sologubenko, E. Felder, K. Giannò, H. R. Ott, A. Vietkine, and A. Revcolevschi, "Thermal conductivity and specific heat of the linear chain cuprate  $\text{Sr}_2\text{CuO}_3$ : Evidence for thermal transport via spinons," *Phys. Rev. B* **62**, R6108 (2001).
- <sup>45</sup>S. Trotzky, P. Cheinet, S. Fölling, M. Feld, U. Schnorrberger, A. M. Rey, A. Polkovnikov, E. A. Demler, M. D. Lukin, and I. Bloch, "Time-resolved observation and control of superexchange interactions with ultracold atoms in optical lattices," *Science* **319**, 295–299 (2008).
- <sup>46</sup>J. Simon, W. S. Bakr, R. Ma, M. E. Tai, P. M. Preiss, and M. Greiner, "Quantum simulation of antiferromagnetic spin chains in an optical lattice," *Nature (London)* **472**, 307–312 (2011).
- <sup>47</sup>Y.-A. Chen, S. Nascimbène, M. Aidelsburger, M. Atala, S. Trotzky, and I. Bloch, "Controlling correlated tunneling and superexchange interactions with ac-driven optical lattices," *Phys. Rev. Lett.* **107**, 210405 (2011).

### ALL BACK ISSUES ARE AVAILABLE ONLINE

The contents of the *American Journal of Physics* are available online. AJP subscribers can search and view full text of AJP issues from the first issue published in 1933 to the present. Browsing abstracts and tables of contents of online issues and the searching of titles, abstracts, etc. is unrestricted. For access to the online version of AJP, please visit <http://aapt.org/ajp>.

Institutional and library ("nonmember") subscribers have access via IP addresses to the full text of articles that are online; to activate access, these subscribers should contact AIP, Circulation & Fulfillment Division, 800–344–6902; outside North American 516–576–2270 or [subs@aip.org](mailto:subs@aip.org).

APPT (individual) members also have access to the American Journal of Physics Online. Not a member yet? Join today <http://www.aapt.org/membership/joining.cfm>. Sign up for your free Table of Contents Alerts at [http://www.ajp.aapt.org/features/toc\\_email\\_alerts](http://www.ajp.aapt.org/features/toc_email_alerts).